

Preclinical evaluation of novel organometallic ^{99m}Tc -folate and ^{99m}Tc -pterotate radiotracers for folate receptor-positive tumour targeting

Cristina Müller¹, Alexander Hohn¹, P. August Schubiger^{1, 2}, Roger Schibli^{1, 2}

¹ Center for Radiopharmaceutical Science ETH-PSI-USZ, Paul Scherrer Institute 5232 Villigen-PSI, Switzerland

² Department of Chemistry and Applied Biosciences of the ETH, Institute for Pharmaceutical Sciences, ETH Hönggerberg, HCI H425, Wolfgang-Pauli-Strasse 10, 8093 Zürich, Switzerland

Received: 11 November 2005 / Accepted: 26 February 2006 / Published online: 9 June 2006

© Springer-Verlag 2006

Abstract. *Purpose:* The folate receptor (FR) is a valuable tumour marker, since it is frequently overexpressed on various cancer types. The purpose of the present study was to pre-clinically evaluate novel site-specifically modified $^{99m}\text{Tc}(\text{CO})_3$ folate (γ -derivative **4**, α -derivative **5**) and pterotate (**6**) conjugates for FR targeting.

Methods: The $^{99m}\text{Tc}(\text{CO})_3$ radiotracers **4–6** were prepared by a kit-like procedure. In vitro characterisation (K_D and B_{max}) of the radiotracers was performed with FR-positive KB cells. Tissue distribution was studied in tumour-bearing mice. SPECT/CT experiments were performed with a dedicated small animal SPECT/CT scanner.

Results: The complexes **4–6** were formed in high yields (>92%). Binding constants of the radiotracers (K_D in nM: **4**: 2.09; **5**: 2.51; **6**: 14.52) were similar to those of ^3H -folic acid (K_D in nM: 7.22). In vivo the folate derivatives showed significantly better tumour uptake (**4**: $2.3 \pm 0.4\%$ ID/g and **5**: $1.2 \pm 0.2\%$ ID/g, 4 h p.i.) than the pterotate derivative (**6**: $0.4 \pm 0.2\%$ ID/g, 4 h p.i.). Clearance of all radiotracers from the blood pool and from non-targeted tissues was efficient (tumour to blood ratio approx. 200–350, 24 h p.i.). FR-positive tissue and organs were successfully visualised via small animal SPECT/CT.

Conclusion: Radiotracers **4–6** are the first $^{99m}\text{Tc}(\text{CO})_3$ tracers prepared via a kit formulation which exhibit full biological activity in vitro and in vivo. Folate derivatives **4** and **5** revealed significantly better pharmacokinetic properties than the pterotate derivative **6**. Promising pre-clinical SPECT results warrant further assessment of $^{99m}\text{Tc}(\text{CO})_3$ radiofolates for detection of FR-positive tumours.

Keywords: Folate receptor – Folate – Pterotate – Tumour targeting – Preclinical studies

Roger Schibli (✉)
Department of Chemistry and Applied Biosciences of the ETH,
Institute for Pharmaceutical Sciences, ETH Hönggerberg,
HCI H425, Wolfgang-Pauli-Strasse 10,
8093 Zürich, Switzerland
e-mail: roger.schibli@psi.ch
Tel.: +41-56-3102837, Fax: +41-56-3102849

Eur J Nucl Med Mol Imaging (2006) 33:1007–1016
DOI 10.1007/s00259-006-0111-9

Introduction

The folate receptor (FR) is a high-affinity, membrane-anchored protein which mediates the transport of folic acid and its conjugates into the cell interior by endocytosis. Excessive need of rapidly dividing malignant cells for folates may be a reason for the frequent overexpression of FRs in various cancer types (e.g. ovarian, endometrial, breast, nasopharyngeal, renal and colorectal cancers) [1–5]. Therefore, folic acid has been identified as the prototype of a “Trojan horse” approach to specific tumour targeting for diagnostic and therapeutic purposes [6, 7]. To date, a number of folate conjugates (e.g. of chemotherapeutic agents [8], antisense oligonucleotides [9], protein toxins [10] and liposomes [11]) have successfully been prepared and evaluated in vitro and in vivo. Various groups are currently developing folate-based radiopharmaceuticals, labelled with diverse diagnostic radionuclides (e.g. $^{66/67/68}\text{Ga}$, ^{111}In , ^{99m}Tc) [12–21].

The development of radiopharmaceuticals for labelling with the “matched pair” $^{99m}\text{Tc}/^{188}\text{Re}$ (^{99m}Tc : 6-h half-life, 140-keV γ -radiation; ^{188}Re : 17-h half-life, 2.12-MeV β^-_{max} -radiation) remains an attractive goal because of the excellent decay of these radionuclides, their low cost and their excellent, carrier-free availability. Moreover, technetium and rhenium share many chemical similarities which potentially enable application of structurally almost identical compounds for either diagnosis or therapy. The group of Leamon and co-workers has recently reported the pre-clinical development of a ^{99m}Tc -radiolabelled folate derivative, ^{99m}Tc -EC20 [20, 21]. Their labelling strategies successfully employed a tetradentate N/S-containing bifunctional chelating system for complexation of the ^{99m}Tc (+V)-oxo core.

Our ongoing research programmes are focussing on the development of organometallic $^{99m}\text{Tc}(\text{I})$ - and $^{188/186}\text{Re}(\text{I})$ -radiolabelled tumour-targeting agents, because Re(I) complexes have proven to be kinetically more inert than Re(V) complexes [22, 23]. Because of the high stability (kinetic inertness) and favourable labelling characteristics, the $^{99m}\text{Tc}/^{188}\text{Re}$ -tricarbonyl approach represents an attractive radiolabelling strategy for the preparation of folate derivatives featuring target-specific activity for diagnosis and therapy [24–28].

Recently, we reported the synthesis of γ -folate (**1**), α -folate (**2**) and pteroate (**3**) derivatives, functionalised with the picolylamine monoacetic acid (PAMA)-chelating system for labelling with $[\text{M}(\text{CO})_3(\text{OH}_2)_3]^+$ ($\text{M} = ^{99m}\text{Tc}$, ^{nat}Re) [29]. In the study presented here, we wished to report on the development of a new and convenient kit preparation of folate and pteroate analogues starting directly from $[\text{Na}][^{99m}\text{TcO}_4]$. In addition, we report the first in vitro and in vivo studies of these three novel, organometallic ^{99m}Tc -folate/pteroate radiotracers in the FR-overexpressing KB cancer cell line and tumour xenografts thereof. Differences between folate and pteroate derivatives with regard to FR-binding properties and pharmacokinetics were analysed. In vivo SPECT/CT studies with the most promising candidate were performed in anaesthetised mice bearing FR-positive KB cell xenografts. These studies clearly unveiled the high potential of this new ^{99m}Tc -based radiofolate for specific visualisation of FR-positive tumour tissue.

Materials and methods

General

PAMA- γ -folate, PAMA- α -folate and PAMA-pteroate conjugates were synthesised as previously reported [29]. $[3',5',7,9\text{-}^3\text{H}]$ Folic acid potassium salt (37 MBq/ml, 888 GBq/mmol) was purchased from Amersham Biosciences (Buckinghamshire, UK). The scintillation solution Ultima Gold, high flash-point LSC-cocktail was purchased from Packard Company (Groningen, the Netherlands). Precursor $[\text{Na}][^{99m}\text{Tc}(\text{OH}_2)_3(\text{CO})_3]^+$ was prepared using the Isolink kit (Mallinckrodt-Tyco, Petten, the Netherlands). $[\text{Na}][^{99m}\text{TcO}_4]$ was eluted from a $^{99}\text{Mo}/^{99m}\text{Tc}$ generator (Mallinckrodt-Tyco, Petten, the Netherlands) with a 0.9% saline solution. KB cells (CCL-17) were purchased from ATCC (American Type Culture Collection, Manassas, USA). Special RPMI cell culture medium (without folic acid, vitamin B₁₂, phenol red) was purchased from Cell Culture Technologies GmbH (Gravesano/Lugano, Switzerland). HPLC analyses were performed on a Merck-Hitachi L-6200A-system equipped with an L-3000 tunable absorption detector, a Berthold LB 508 radiometric detector and an XTerra (Waters) MS C-18 reversed phase column (5 μm , 15 cm \times 4.6 mm). HPLC solvents: aqueous 0.05 M triethylammonium phosphate buffer, pH 7.0 (solvent A), methanol (solvent B). The HPLC system started with 100% A with a linear gradient to 20% A and 80% B over 15 min, followed by 5 min of 100% A with a flow rate of 1 ml/min. Radioactivity (γ -radiation of ^{99m}Tc) was measured with a γ -counter (Cobra II, Model B 5003, Packard) and (β -radiation of ^3H) with a β -counter (TRI-CARB, 1900 TR, Liquid Scintillation Analyzer, Packard). Protein concentrations for the in vitro experiments were measured with a microplate reader (Bio-Rad, Model 550), using a Micro BCA Protein Assay kit (Prod # 23235), Socochim. A combined small-animal SPECT/CT device (X-SPECT, Gamma Medica Inc.,

Northridge, CA, USA) with a single-head SPECT camera and CT detector was used for in vivo imaging.

Cell cultures

KB cells (human nasopharyngeal carcinoma cell line) were cultured continuously in 150-cm² flask as monolayers at 37°C in a humidified atmosphere containing 7.5% CO₂. The cells were propagated in folate-deficient special RPMI 1640 medium (FFRPMI: modified RPMI 1640 medium without folic acid, vitamin B₁₂ and phenol red), supplemented with 10% heat-inactivated fetal calf serum (FCS, as the only source of folate), L-glutamine and antibiotics (penicillin 100 IU/ml, streptomycin 100 $\mu\text{g}/\text{ml}$, fungizone 0.25 $\mu\text{g}/\text{ml}$). Cell culture media such as FCS-supplemented FFRPMI are known to feature a final folate concentration of ~ 3 nM, i.e. a value at the low end of the physiological concentration in human serum [30]. Cell preparation for in vitro experiments was as follows: 18–20 h prior to each experiment, the cells were seeded in 12-well plates ($\sim 8 \times 10^5$ cells/well) and incubated at 37°C to form confluent monolayers overnight. Experiments were performed in triplicate for each point in time and/or concentration. Cell preparation for in vivo experiments was as follows: For subcutaneous inoculation of the mice, subconfluent cells were harvested by treatment with EDTA (1 mM) in phosphate-buffered saline (PBS, 1 \times , pH 7.4). The cells were then washed once with PBS and pelleted by spinning at 1,000 $\times g$ for 5 min at 20°C. The cells were resuspended in PBS to a final concentration of 50×10^6 cells/ml.

Preparation of the radiotracers 4–6

$^{99m}\text{Tc}(\text{CO})_3$ -PAMA- γ -folate (**4**), $^{99m}\text{Tc}(\text{CO})_3$ -PAMA- α -folate (**5**) and $^{99m}\text{Tc}(\text{CO})_3$ -PAMA-pteroate (**6**) radiotracers were prepared according to the following general procedures: In *method I* a neutral solution of *fac*- $[\text{Na}][^{99m}\text{Tc}(\text{OH}_2)_3(\text{CO})_3]^+$ (100 μl), PBS (pH 7.4, 350 μl) and a stock solution of the corresponding derivative (**1–3**, 50 μl , 10^{-3} M in PBS) were mixed in a sealed glass vial. The reactions were heated for 30 min at 75°C to form the corresponding complexes **4–6** in excellent yields (>95%). In *method II* the derivatives **1–3** (0.1 μmol) and the components of the Isolink kit (4.5 mg Na₂[H₃-BCO₂], 2.9 mg B₄Na₂O₇, 7.8 mg Na₂CO₃, 9.0 mg NaK₂C₄H₄O₆·4H₂O) were placed in a sealed glass vial. 1 ml $[\text{Na}][^{99m}\text{TcO}_4]$ was added. After 45-min reaction time at 100°C, the vial was cooled on ice and neutralised with 0.2 ml of a 1:2 mixture of 1 M phosphate buffer (pH 7.4) and 1 M HCl. $^{99m}\text{Tc}(\text{CO})_3$ complexes **4–6** were formed at a yield of >92%. The radiolabelled complexes **4–6** were separated from unlabelled compounds **1–3** by high-performance liquid chromatography (HPLC). Due to HPLC purification, the specific activities of radiotracers **4–6** can be considered identical with that of ^{99m}Tc in the generator eluate, 26 h post elution (approx. 5.02 TBq/ μmol). The solutions were further diluted to a final concentration of 1 MBq/ml for in vitro experiments or 3.7 MBq/ml for in vivo experiments. For SPECT experiments with complex **4**, solutions were prepared with a radioactivity of 3 GBq/ml.

Time-dependent cell uptake

Cell binding experiments with radiotracers **4–6** were performed according to the following general procedure: cell monolayers were rinsed twice with ice-cold PBS (pH 7.4). Pure FFRPMI medium (without FCS/L-glutamine/antibiotics, 975 μl) was added to each well. The well plates were pre-incubated at 37°C for 10 min. A

solution of the respective radiotracer **4–6** (25 μ l, 1 MBq/ml) was added and the well plates were incubated again at 37°C for 5, 15, 30, 60, 120 and 240 min. After the corresponding incubation period the monolayers were washed several times. Counted radioactivity in samples, washed with PBS (pH 7.4) only, could be ascribed to the sum of FR-bound radiotracer on the cell surface and the internalised fraction. Cell samples, washed with stripping buffer (aqueous solution of 0.1 M acetic acid and 0.15 M NaCl, pH 3) in order to release radiotracer from FRs on the cell surface, enabled the determination of the internalised fraction of radioactivity [31, 32]. In this way, it was possible to distinguish between total bound radiotracer and the internalised fraction. The cell monolayers were lysed in 1 N NaOH (1 ml), transferred to 4-ml tubes and homogenised by vortex. Each sample was counted for radioactivity with a γ -counter, using reference counts from samples which contained the total amount of originally added radioactivity. The concentration of proteins was determined for each sample using a Micro BCA Protein Assay kit in order to normalise measured radioactivity in each sample with respect to the averaged sample protein content. The raw data of measured radioactivity corresponded to the sum of bound and internalised radioactivity or internalised radioactivity only. The data were converted from counts per minute (cpm) per mg protein into percentage of total added radioactivity.

Determination of K_D and B_{max} of compounds **4–6** and ^3H -folic acid

The experiments were performed at 4°C in order to attenuate endocytosis. Since addition of excess folic acid resulted in <0.5% residual radioactivity (data not shown), non-specific binding of the radiotracers could be neglected. Inhibition experiments with the folate and pterate radiotracers **4–6** and ^3H -folic acid were performed according to the following procedure: The monolayers were rinsed twice with ice-cold PBS (pH 7.4). Pure ice-cold FFRPMI medium (without FCS/L-glutamine/antibiotics, 475 μ l) was added to each well. Then, 500 μ l of the corresponding ice-cold folic acid solution (ten different concentrations from 0.001 μ M to 0.2 μ M, prepared in PBS, pH 7.4) was added. The well plates were pre-incubated at 4°C for 40 min. A solution of the corresponding radiotracer **4–6** (25 μ l, 1 MBq/ml) or ^3H -folic acid (25 μ l, ~19 kBq) was added and the well plates were incubated again at 4°C for 2 h. The monolayers were washed three times with PBS (pH 7.4). The cell monolayers were lysed in 1 N NaOH (1 ml), transferred to 4-ml tubes and homogenised by vortex. The concentration of proteins was determined for each sample by a Micro BCA Protein Assay kit. Samples of radiotracers **4–6** were counted for radioactivity with a γ -counter and samples of ^3H -folic acid were, after mixing with a scintillation solution, counted in a β -counter. K_D and B_{max} values were determined by converting the raw data of measured radioactivity from cpm bound per mg protein into pmol radiotracer bound per mg protein and analysed by Rosenthal plot. The mean values for K_D and B_{max} of each radiotracer (**4–6**) and ^3H -folic acid, acquired in two independent experiments, are shown in Table 1. The values

shown in parentheses represent the lower and upper limits of the 95% confidence interval.

Dissociation and externalisation experiment

Dissociation and externalisation studies of the radiotracer **4** were performed according to the following procedure: The monolayers were rinsed twice with ice-cold PBS (pH 7.4). Pure FFRPMI medium (without FCS/L-glutamine/antibiotics, 975 μ l) was added to each well and the well plates pre-incubated at 37°C for 10 min. A solution of the radiotracer **4** (25 μ l, 1 MBq/ml) was added to each well and the well plates incubated for 2 h at 37°C. The cell monolayers were then washed with either PBS or stripping buffer ($t=0$) [31, 32]. Pure FFRPMI medium (without FCS/L-glutamine/antibiotics, 1 ml) was added to each well and the well plates were incubated again for 2 h at 37°C ($t=2$ h). After washing the cells as described above, fresh FFRPMI medium (without FCS/L-glutamine/antibiotics, 1 ml) was again added to each well. The cells were incubated for another 3 h ($t=5$ h). This procedure was repeated after an incubation period of 12 h ($t=17$ h). Each of the supernatants, combined with the corresponding wash solutions, was transferred to a 4-ml tube and counted for radioactivity. Counts measured in each sample were analysed and expressed as percentage of the sum of total cell-bound and internalised radioactivity at $t=0$ (100%).

In vivo studies

Four- to 5-week-old female, athymic nude mice (CD1-Foxn1/nu) were purchased from Charles River Laboratories (Sulzfeld, Germany). Mice were housed under conditions of controlled temperature (26°C), humidity (68%) and daily light cycle (12 h light/12 h dark). The animals were fed with a folate-deficient rodent chow in order to reduce their serum folate to a level near that of human serum [13]. After an acclimation period of 5–7 days, the mice were inoculated subcutaneously with 0.1 ml tumour cell suspension (50×10^6 cells/ml) into the subcutis of the axilla. Radiotracer distribution studies were performed 12–14 days after tumour cell inoculation. Radiotracers **4–6** (approx. 370 kBq per mouse) were administered via a lateral tail vein. To competitively block tissue FRs, mice were injected with excess folic acid (0.25 μ mol in PBS pH 7.4) 5 min prior to administration of the radiotracer. At the indicated points in time the animals were sacrificed and dissected. The selected tissues were removed and weighted, and the radioactivity was counted by a γ -counter to determine tissue distribution of the radiotracers within the test animal. In vivo biodistribution studies were performed in triplicate for each radiotracer (**4–6**) and time point. The results were tabulated as percentage of the injected dose per gram of tissue (% ID/g), using reference counts from a definite sample of the original injectate.

Table 1. Binding constants of radiotracers **4–6** and ^3H -folic acid in KB cells, determined by Rosenthal analysis

Radiotracer	B_{max} (pmol/mg protein)	K_D (nM)
$^{99m}\text{Tc}(\text{CO})_3\text{-PAMA-}\gamma\text{-folate}$ (4)	14.7 (–22.1 to +51.5)	2.09 (–11.5 to +15.7)
$^{99m}\text{Tc}(\text{CO})_3\text{-PAMA-}\alpha\text{-folate}$ (5)	6.0 (+3.4 to +8.7)	2.51 (–6.2 to +11.2)
$^{99m}\text{Tc}(\text{CO})_3\text{-PAMA-pterate}$ (6)	7.7 (–1.5 to +16.9)	14.52 (–16.7 to +45.8)
^3H -folic acid	11.9 (–12.2 to +36.0)	7.22 (–11.2 to +25.6)

Values shown in parentheses represent the lower and upper limits of the 95% confidence interval; number of experiments =2

Imaging experiments were performed 24 h p.i. of radiotracer **4**. The radiotracer (approx. 550 MBq) was administered via a lateral tail vein. The mice were anaesthetised with an isoflurane/oxygen mixture. Depth of anaesthesia was monitored by measuring respiratory frequency using a respiratory belt. Body temperature was controlled by a rectal probe and kept at 37°C by a thermocoupler and a heated air stream. SPECT data were acquired and reconstructed by software LumaGEM (version 5.407 lum 10). CT data were acquired by the manufacturer's software and reconstructed with the software COBRA (version 4.5.1). Fusion of SPECT and CT data was performed by software IDL Virtual Machine (version 6.0). Images were generated by software Amira (version 3.1.1).

Results

Synthesis of the radiotracers

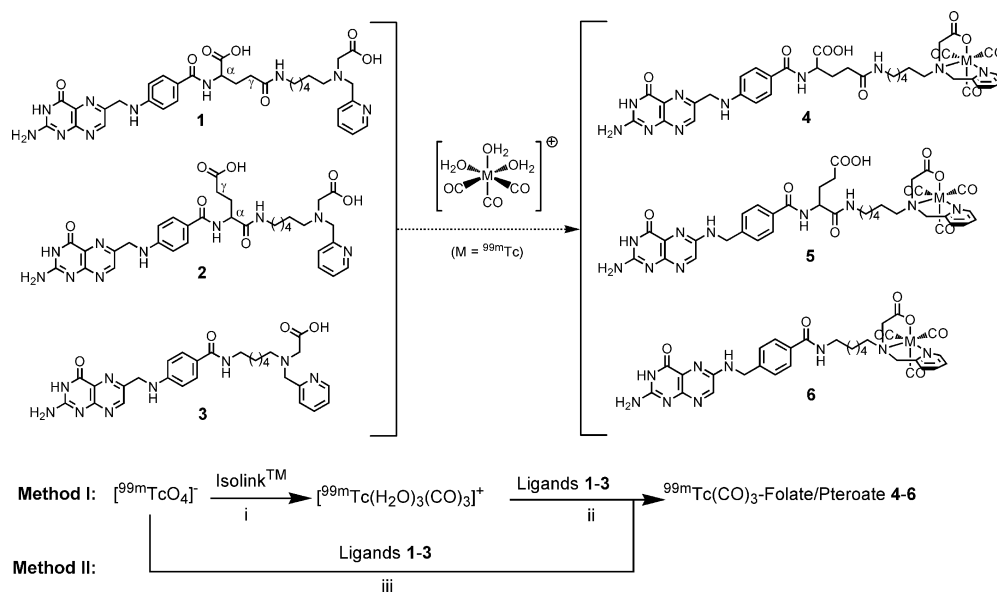
Radiolabelling of ligands **1–3** was performed either by the two-step (method I) or a new, one-step, kit-like procedure (method II, Fig. 1). For method I, the precursor $[\text{}^{99\text{m}}\text{Tc}(\text{CO})_3(\text{OH}_2)_3]^+$ was prepared first by the Isolink kit, followed by neutralisation with phosphate/HCl buffer. Then, the precursor was added to a solution of the corresponding derivatives **1–3** in PBS. After heating at 75°C for 30 min, the complexes **4–6** were formed almost quantitatively (>95% yield) [29]. For method II, the folate precursors **1–3** (0.1 μmol) were placed together with the Isolink components in a 10-ml vial, sealed and flushed with nitrogen. After addition of 1 ml of $[\text{}^{99\text{m}}\text{TcO}_4]^-$ the reactions were heated for 45 min at 100°C followed by neutralisation (Fig. 1). The formation of radiotracers **4–6** was observed in excellent yields (>92%), comparable to the data obtained by the two-step reaction. The amount of (unidentified) byproducts ranged between 2% and 8% of the total radioactivity

for both methods. Also the HPLC traces of the non-radioactive precursors **1–3** (observed at $\lambda=254$ nm), analysed after the labelling reaction, revealed only minor formation of non-radioactive byproducts (Fig. 2). This proved the high stability of the folate precursors even under reductive and basic reaction conditions and hence their suitability for an Isolink adapted kit formulation. Tridentate coordination of the $[\text{}^{99\text{m}}\text{Tc}(\text{CO})_3]^+$ core to ligands **1–3** resulted in a significant shift in the HPLC retention times (**4, 5**: $R_t=15.5$ min and **6**: $R_t=16.5$ min) compared with those of the free ligands **1–3** (**1, 2**: $R_t=11.5$ min and **3**: $R_t=12.5$ min) (Fig. 2). This enabled the clear separation and purification of radiotracers **4–6** from non-radioactive precursors **1–3** in order to achieve high specific activities necessary for in vitro and in vivo studies. High stability of radiotracers **4–6** in PBS as well as in human plasma has been previously tested and proven [29].

In vitro studies

Binding and internalisation studies were performed at 37°C over a period of 4 h (Fig. 3). The sum of FR-bound radiotracers **4–6** and the internalised fractions was calculated as percentage of total added radioactivity, determined by residual cell-associated radioactivity after washing the monolayers with PBS (pH 7.4) [33]. The internalised fractions of the radiotracers **4–6** were ascribed to the radioactivity, measured after washing the cells with stripping buffer (pH 3). No significant differences could be observed between the folate radiotracers **4** and **5** and the pteroate derivative **6**. After 4-h incubation at 37°C, 40–60% of total radioactivity was bound, of which 25–35% was internalised. The results obtained for the folate conjugates **4** and **5** and the pteroate conjugate **6** were within the same range. Blocking experiments were carried out with cells which were pre-incubated with excess folic acid (100 μM) for

Fig. 1. Structure and preparation of novel organometallic $^{99\text{m}}\text{Tc}$ radiofolate and pteroate derivatives via a two-step and a one-step, kit formulation: i) 20 min, 100°C, neutralisation; ii) 30 min, 75°C; iii) $\text{Na}_2[\text{H}_3\text{BCO}_2]$, $\text{B}_4\text{Na}_2\text{O}_7$, Na_2CO_3 , $\text{NaKC}_4\text{H}_4\text{O}_6$, 45 min, 100°C, neutralisation



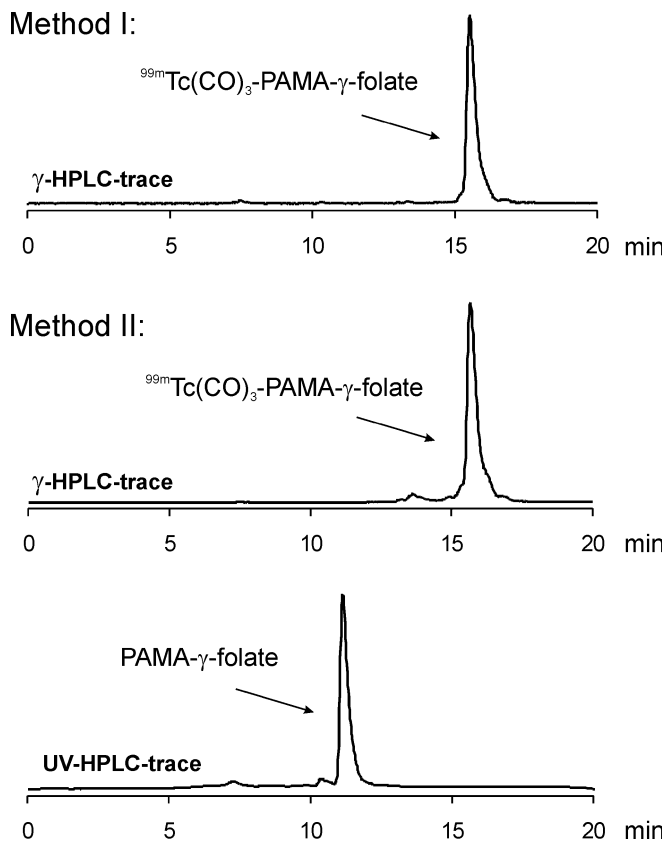


Fig. 2. Representative γ -HPLC traces of complex **4** prepared with $[\text{}^{99\text{m}}\text{Tc}(\text{CO})_3(\text{OH}_2)_3]^+$ in two steps (method I) and prepared in a single step using $[\text{}^{99\text{m}}\text{TcO}_4]^-$ directly (method II); UV-HPLC trace of unlabelled folate precursor **1**

40 min before addition of radiotracers **4–6**. Under these conditions less than 0.5% of total added radioactivity was bound to the cells (data not shown). These experiments proved the high specificity of the derivatives **4–6** for the targeted FRs in vitro and negligible non-specific binding of the radiofolates.

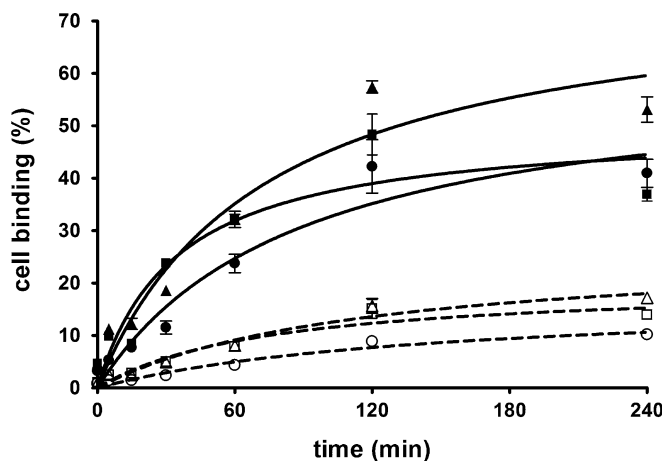


Fig. 3. Time-dependent binding (\blacksquare **4**, \blacktriangle **5**, \bullet **6**) and internalisation (\square **4**, \triangle **5**, \circ **6**) of the radiotracers **4–6** to FRs of KB cancer cells, incubated at 37°C

K_D and B_{max} values of the radiotracers **4–6** and ^3H -folic acid were determined by incubation of the radiotracers and cold folic acid with KB cells for 2 h at 4°C . Since non-specific cell binding was negligible and because endocytosis was inhibited at 4°C , radioactivity detected in the samples could be ascribed to specific cell surface-bound radiotracer. K_D values and B_{max} values of the folate **4** and **5** and pteroate **6** derivatives and the parent ligand ^3H -folic acid are summarised in Table 1. K_D values were observed in the low nM range, comparable to that of ^3H -folic acid. B_{max} values of compounds **4–6** ranged between 6.0 and 14.7 pmol/mg protein (95% confidence interval -22.1 to $+51.5$) and were similar to that found for the parent ligand ^3H -folic acid (11.9 pmol/mg protein, 95% confidence interval -12.2 to $+36.0$).

Representative for all three organometallic radiotracers **4–6**, dissociation of compound **4** from FRs on the cell surface and externalisation were investigated. Radiotracer **4** was incubated with KB cells for 2 h at 37°C , followed by washing steps with PBS for determination of total bound and internalised radioactivity, or with stripping buffer in order to define the acid-resistant (internalised) fraction (see [Materials and methods](#)). Overall dissociation and externalisation of radioactivity was less than 10% after 17 h.

In vivo studies

Radiotracers **4–6** were tested for their ability to bind to FR-positive tumour tissue in vivo. Athymic nude mice, bearing KB cell tumour xenografts, were used for biodistribution studies performed 1 h, 4 h and 24 h post injection of the radiotracers (Tables 2, 3 and 4). Compounds **4–6** accumulated in FR-positive tissues, namely the tumours and the kidneys. The tumour uptake 4 h p.i. was highest for the γ -derivative **4** ($2.33 \pm 0.36\%$ ID/g), significantly lower for the α -derivative **5** ($1.24 \pm 0.19\%$ ID/g, $p < 0.018$) and even more reduced for the pteroate derivative **6** ($0.43 \pm 0.17\%$ ID/g, $p < 0.005$). Clearance from the bloodstream was fast, resulting in marginal amounts of radioactivity as early as 1 h post injection of the radiotracers (**4**: $0.09 \pm 0.02\%$ ID/g; **5**: $0.08 \pm 0.04\%$ ID/g; **6**: $0.06 \pm 0.01\%$ ID/g) without significant differences amongst the compounds ($p > 0.05$). Radioactivity found in organs such as heart, lung, spleen, muscle and bone was negligible as well. Twenty-four hours after injection of the radiotracers, tumour-to-blood ratios reached values between 200 and 350 for all compounds (**4–6**: $p > 0.05$). Apart from in the tumours, a significant amount of radioactivity was found only in the kidneys (**4**: $18.5 \pm 0.7\%$ ID/g; **5**: $12.4 \pm 1.9\%$ ID/g; **6**: $3.3 \pm 0.4\%$ ID/g, 4 h p.i.). It is noteworthy that again (i.e. as observed in tumours) the pteroate derivative **6** showed lower uptake in kidneys than did the folate derivatives. While absolute tumour and kidney uptake differed among the radiotracers **4–6** ($p < 0.05$), tumour-to-kidney ratios were similar ($p > 0.05$) over time for all complexes (**4**: 0.13 ± 0.02 ; **5**: 0.10 ± 0.00 ; **6**: 0.13 ± 0.05 ; 4 h p.i.). Co-administration of folic acid ($0.25 \mu\text{mol}$) 5 min prior to radiotracer injection resulted in an almost complete blockade of FRs in the tumour and

the kidneys, giving rise to very low accumulation of radioactivity (tumour: <0.05% ID/g; kidneys: <0.4% ID/g, 4 h p.i.). Biodistribution of the complexes **4–6** in other organs and tissue were not or only marginally affected under blockade conditions, proving the specificity of folate-based radiotracers.

SPECT/CT studies were performed in order to visualise the distribution of the radiotracer in a living animal. For that reason, mice were injected with approximately 550 MBq of complex **4** and scanned 24 h later. This time point was determined as the most favourable for imaging purposes since the main abundance of radioactivity had been cleared from non-targeted tissues. For the present experiment, the animal was scanned for 30 min using a low-resolution/high-sensitivity parallel collimator. Accumulation of radioactivity was unambiguously detected in tumours and kidneys as well as in the gastrointestinal tract (Fig. 4a,b). The same animal was used for studies under FR-blocked conditions (0.25 μmol folic acid, administered 5 min prior to the radiotracer). These experiments allowed detection of radioactivity neither in the tumour tissue nor in the kidneys, but only non-specifically distributed in the gastrointestinal tract (Fig. 4c,d). It is important to recognise that application of significantly higher amounts of radioactivity/radiotracer compared with ex vivo biodistribution studies (by a factor of $\sim 1,000$) had no influence on FR-mediated and non-specific tracer uptake in mice. Post-mortem results regarding tissue distribution of radioactivity (% ID/g) in animals injected with the amount of radiotracer **4** used for SPECT scans were in agreement with those found in the previous time-dependent biodistribution studies, as shown in Table 2.

Discussion

We have previously shown that folate and pterate derivatives can be efficiently radiolabelled with the organ-

ometallic precursor $[\text{}^{99\text{m}}\text{Tc}(\text{CO})_3(\text{OH}_2)_3]^+$ when functionalised with the tridentate PAMA-chelating system [29]. In the present study, to address the potential routine application of the new radiofolates/pteroates in a clinical setting, we investigated the feasibility of a one-step preparation of the corresponding compounds based on the Isolink kit. Of particular concern was the question of whether the ligands and their functional groups would be resistant to the harsh, reductive labelling conditions necessary to convert Tc(+VII) to Tc(+I). The results of our experiments demonstrated that both folate and pterate derivatives **1–3** (and their functional groups) are sufficiently resistant to the reductive component ($\text{Na}_2[\text{H}_3\text{BCO}_2]$) of the Isolink kit. Hence, we could prove that the radiolabelling and the formation of the desired radiotracers can be efficiently achieved at low concentrations of the organic folate/pteroate precursors, giving rise to high specific activity starting directly from $[\text{}^{99\text{m}}\text{TcO}_4]^-$. No traces of free metal precursor or $[\text{}^{99\text{m}}\text{TcO}_4]^-$ were detectable after the reactions. The yields found for the kit preparation were only marginally reduced compared with those obtained by the classical two-step radiolabelling procedure. The amounts of folate/pteroate derivative (approx. 0.1 μmol) used for the labelling with the $^{99\text{m}}\text{Tc}$ -tricarbonyl core were comparable to those reported by Leamon and co-workers for the preparation of $^{99\text{m}}\text{Tc}$ -EC20 (0.13 μmol) [20, 21].

Binding constants (K_D , B_{max}) of the radiotracers **4–6** revealed retention of FR affinity in vitro compared with ^3H -folic acid, regardless of the position of derivatisation (γ - vs α -carboxylate group) and absence of the glutamate moiety, when tested in KB cells. A slightly increased K_D value of the pterate derivative **6**, compared with the folate derivatives **4** and **5**, might indicate a tendency for pterate derivatives to show decreased FR affinity. However, these differences are marginal and not significant. Our findings are in agreement with those reported by Leamon et al., who performed similar studies with α - and γ -folate conjugates of non-radioactive macromolecules [34]. They found that

Table 2. Time-dependent bio-distribution of $^{99\text{m}}\text{Tc}(\text{CO})_3$ -PAMA- γ -folate (**4**) using KB tumour xenografts in athymic nude mice

	$^{99\text{m}}\text{Tc}(\text{CO})_3$ -PAMA- γ -folate (4)			Folic acid (0.25 μmol)
	1 h	4 h	24 h	4 h
Blood	0.09 \pm 0.02	0.04 \pm 0.00	0.01 \pm 0.02	0.01 \pm 0.00
Heart	0.85 \pm 0.27	0.32 \pm 0.07	0.02 \pm 0.00	0.00 \pm 0.00
Lung	0.57 \pm 0.19	0.33 \pm 0.02	0.03 \pm 0.02	0.02 \pm 0.02
Spleen	0.20 \pm 0.03	0.15 \pm 0.04	0.01 \pm 0.02	0.01 \pm 0.01
Kidney	14.37 \pm 1.35	18.48 \pm 0.72	6.90 \pm 0.72	0.06 \pm 0.01
Stomach	0.31 \pm 0.06	0.63 \pm 0.33	3.70 \pm 6.37	3.80 \pm 5.46
Intestines	1.89 \pm 0.37	1.49 \pm 0.23	0.76 \pm 1.15	0.40 \pm 0.45
Contents of intestines	9.31 \pm 5.94	38.51 \pm 55.88	7.08 \pm 11.52	5.54 \pm 3.38
Liver	0.89 \pm 0.31	2.37 \pm 2.85	0.10 \pm 0.02	0.12 \pm 0.02
Muscle	1.06 \pm 0.33	0.54 \pm 0.05	0.05 \pm 0.04	0.04 \pm 0.01
Bone	0.76 \pm 0.22	0.31 \pm 0.07	0.03 \pm 0.04	0.01 \pm 0.01
Tumour	1.30 \pm 0.61	2.33 \pm 0.36	1.32 \pm 0.17	0.00 \pm 0.01
Tumour-to-blood ratio	15.82 \pm 11.29	58.0 \pm 12.2	255.4 \pm 115.4	
Tumour-to-liver ratio	1.60 \pm 0.81	2.53 \pm 2.13	13.77 \pm 1.90	
Tumour-to-kidney ratio	0.09 \pm 0.05	0.13 \pm 0.02	0.19 \pm 0.04	

Values (% ID/g) represent the mean \pm SD of data from three animals per cohort

Table 3. Time-dependent bio-distribution of the $^{99m}\text{Tc}(\text{CO})_3$ -PAMA- α -folate (**5**) using KB tumour xenografts in athymic nude mice

	$^{99m}\text{Tc}(\text{CO})_3$ -PAMA- α -folate (5)			Folic acid (0.25 μmol)
	1 h	4 h	24 h	4 h
Blood	0.08±0.04	0.07±0.08	0.01±0.01	0.01±0.01
Heart	0.39±0.01	0.15±0.12	0.02±0.01	0.01±0.01
Lung	0.30±0.01	0.15±0.14	0.02±0.01	0.02±0.01
Spleen	0.09±0.02	0.06±0.06	0.00±0.00	0.01±0.01
Kidney	18.18±1.80	12.36±1.86	9.74±0.96	0.25±0.26
Stomach	0.78±0.19	0.47±0.13	0.63±0.67	0.11±0.07
Intestines	23.55±30.37	0.88±0.34	0.08±0.06	0.34±0.22
Contents of intestines	197.6±186.6	5.50±4.94	1.10±0.95	4.37±3.62
Liver	7.23±2.26	0.79±0.92	0.15±0.02	0.81±0.38
Muscle	0.44±0.04	0.17±0.05	0.03±0.01	0.22±0.34
Bone	0.29±0.09	0.47±0.58	0.01±0.01	0.38±0.66
Tumour	3.56±0.53	1.24±0.19	1.87±0.27	0.03±0.02
Tumour-to-blood ratio	49.32±23.56	31.44±51.16	335.1±386.0	
Tumour-to-liver ratio	0.55±0.28	1.80±1.72	12.77±2.18	
Tumour-to-kidney ratio	0.20±0.01	0.10±0.00	0.19±0.04	

Values (% ID/g) represent the mean±SD of data from three animals per cohort

γ -glutamyl- and α -glutamyl-linked derivatives were able to bind to FR-positive cells at virtually identical levels. Also, a pterate derivative revealed comparable properties. Based on our and other groups' results, one can conclude that selective isomeric conjugation (via the γ - or the α -carboxylate group) is not required, and that the presence of glutamic acid is not essential for FR binding. On the other hand, our results suggest that absence of the glutamic acid moiety has a significant influence on the in vivo biodistribution of our organometallic pterate tracer **6** (vide infra).

The amount of in vitro cell binding was similar for derivatives **4–6** over the investigated period of 4 h. The fraction of FR-specifically associated radiotracer continuously increased until reaching a steady state after approx. 2 h (Fig. 3). Washing the cells with stripping buffer (pH 3) enabled release of FR-bound radiotracer on the cell surface

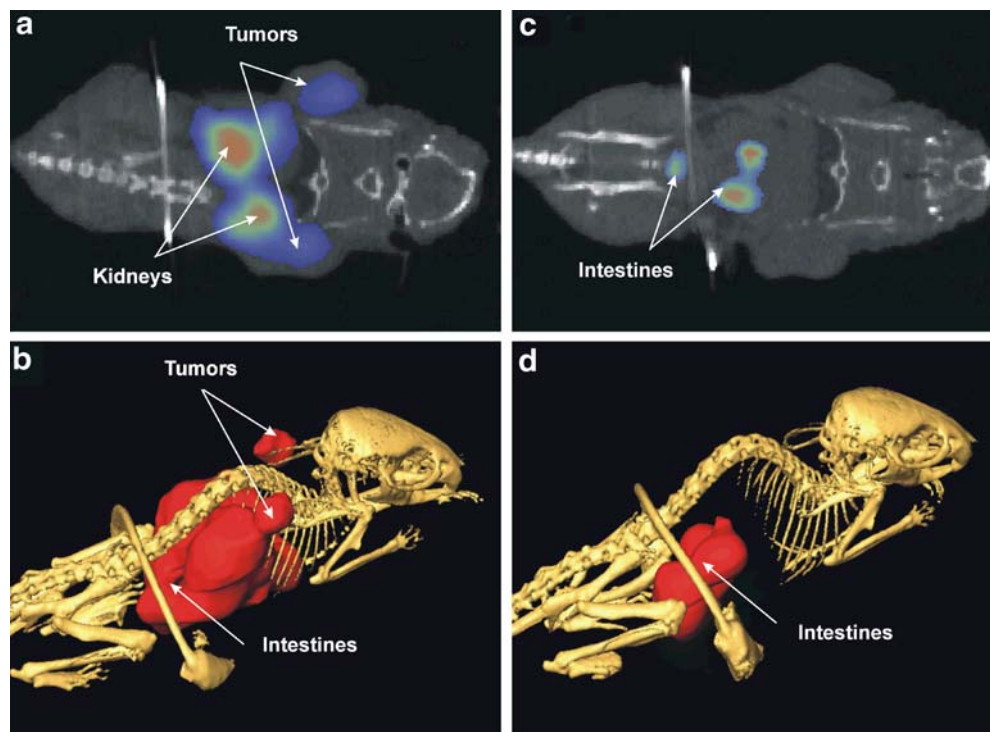
[5, 31, 32, 35]. Interestingly, the acid-resistant fraction ascribed to internalised radiotracers of about 30% remained almost constant over the whole period of 4 h. This indicates that most of the FRs (about 70%) remained permanently cell surface exposed and were not internalising when targeted with the radiotracers. These findings are in agreement with those of Paulos et al., who recently reported for several cell lines that only approximately 25% of the total cell-associated radioactivity had been internalised after 6 h [36]. Their and our data indicate a slow time response of radiotracer/FR endocytosis and potential recycling of the FRs. However, these processes are not yet completely understood and might vary among different cell lines depending on their level of FR expression as well as the kinetics of FR-mediated uptake of folate-based pharmaceuticals [15, 37, 38]. The slow turnover rate of the FRs might be an unfavourable characteristic for

Table 4. Time-dependent bio-distribution of the $^{99m}\text{Tc}(\text{CO})_3$ -PAMA-pterate (**6**) using KB tumour xenografts in athymic nude mice

	$^{99m}\text{Tc}(\text{CO})_3$ -PAMA-pterate (6)			Folic acid (0.25 μmol)
	1 h	4 h	24 h	4 h
Blood	0.06±0.01	0.10±0.02	0.00±0.00	0.04±0.00
Heart	0.06±0.01	0.07±0.02	0.02±0.01	0.02±0.00
Lung	0.13±0.07	0.16±0.02	0.02±0.01	0.06±0.02
Spleen	0.12±0.16	0.06±0.00	0.01±0.01	0.02±0.01
Kidney	6.10±1.30	3.30±0.41	2.08±0.32	0.37±0.05
Stomach	0.95±0.70	8.47±9.94	0.30±0.18	25.44±44.00
Intestines	8.43±5.65	0.65±0.31	0.06±0.05	0.17±0.07
Contents of intestines	302.1±427.1	5.79±2.99	0.48±0.57	1.22±1.21
Liver	4.19±1.85	1.32±0.27	0.47±0.20	1.62±0.14
Muscle	0.08±0.05	0.05±0.03	0.02±0.02	0.01±0.00
Bone	0.09±0.10	0.03±0.01	0.03±0.01	0.01±0.00
Tumour	0.22±0.08	0.43±0.17	1.05±0.33	0.01±0.00
Tumour-to-blood ratio	3.45±0.62	4.51±1.53	217.2±40.1	
Tumour-to-liver ratio	0.06±0.05	0.33±0.10	2.33±0.34	
Tumour-to-kidney ratio	0.04±0.01	0.13±0.05	0.52±0.21	

Values (% ID/g) represent the mean±SD of data from three animals per cohort

Fig. 4. An athymic nude mouse with two KB tumours on the right and left shoulder (*arrows*) was scanned 24 h after radio-tracer injection (**a,b**) and 24 h later under blockade conditions (0.25 μmol cold folic acid injected 5 min prior to the radio-tracer) (**c,d**). Both SPECT/CT scans lasted for 30 min. The SPECT images represent a coronal whole-body section through the KB tumours and through the kidneys (**a,c**) as well as a whole-body SPECT/CT image (**b,d**)



effective tumour uptake of folate-based (radio)pharmaceuticals. However, the *in vitro* experiments clearly showed that the radiofolate complexes, even if not internalised, remained FR-specifically and stably bound on the cell surface over several hours.

In vivo experiments revealed significant differences for absolute tumour uptake between the folate derivatives **4** and **5** and the pteroate derivative **6**. For complexes **4** and **5** we found maximal uptake in the tumour tissue between 1 and 4 h after administration (approx. 2–3% ID/g). Fast clearance from the blood pool could be found with all complexes. These observations were supported by data of other groups, suggesting that *in vivo* half-lives of most folate conjugates in circulation were <5 min, predominately because of their rapid clearance via kidneys [20, 39]. Although fast and effective renal elimination is a highly desirable feature for radiopharmaceuticals, in the case of folate derivatives it leads to specific and relatively high renal accumulation of radioactivity owing to physiological FR expression in this tissue [40–43]. We also found relatively high amounts of radioactivity in the intestines, which might be attributed to substantial and efficient hepatobiliary excretion of our radiotracers. It is noteworthy that radioactivity was found in the intestinal contents, but not in the intestinal tissue itself or in the liver. Interestingly, hepatobiliary clearance of other folate and pteroate radiotracers was reported to be negligible [20, 44–46]. On the other hand, biodistribution data and particularly tumour-to-background ratios of radiotracers **4** and **5** were largely comparable to and competitive with those of other folate radiotracers reported in the literature, such as $^{99\text{m}}\text{Tc}$ -HYNIC-folate, $^{99\text{m}}\text{Tc}(\text{CO})_3$ -DTPA-folate and $^{99\text{m}}\text{Tc}$ -DTPA-folate, but also (pre)clinically evaluated folate

radiopharmaceuticals such as ^{111}In -DTPA-folate and $^{99\text{m}}\text{Tc}$ -EC20 [16, 20, 21, 33, 44, 45]. What we found, however, was that the pteroate derivative **6** revealed a significantly inferior tumour accumulation compared with the folate derivatives **4** and **5**. These results were somewhat surprising since the *in vitro* data entailed similar binding affinity amongst the folate and pteroate derivatives. The implications of the glutamate moiety for the pharmacokinetics of our radiofolates need to be further investigated. It is evident that the folate derivatives possess more favourable pharmacokinetic features than the pteroate derivative. Finally, FR specificity of all three radiotracers **4–6** was unambiguously proven by co-administration of excess folic acid, which resulted in almost complete inhibition of the radiotracer uptake in the FR-positive tissue and organs.

Representatively for all three radiotracers, the γ -folate derivative **4** was further evaluated *in vivo* using a dedicated small-animal, single-detector SPECT/CT device. SPECT/CT scans were successfully conducted with an anaesthetised mouse bearing KB tumour xenografts. The same animal was successfully used for blockade experiments employing radiotracer **4** and excess non-radioactive folic acid. The SPECT images clearly confirmed the specificity of radiotracer **4** for the FR. Owing to the intrinsic low tumour uptake of all three radiotracers (<2.5% ID/g) and at the same time a large portion of radioactivity in the intestinal contents, it was difficult to clearly delineate different organs and tissue at early time points after injection (1–4 h p.i.). Significantly better data were obtained at late time points (24 h p.i.) but this restriction obliged us to inject relatively high doses of radioactivity (up to 550 MBq/mouse).

In summary, in this study we were able to demonstrate that a “one-pot” kit-like preparation of organometallic ^{99m}Tc radiotracers which display in vitro and in vivo retention of receptor-binding capacity is possible. The novel $^{99m}\text{Tc}(\text{CO})_3$ -folate and the $^{99m}\text{Tc}(\text{CO})_3$ -pteroate radiotracers were able to specifically target FR-positive tumours as well as other FR-positive tissues. Particularly the folate derivatives revealed excellent target specificity and pharmacokinetic properties in vivo. Originally, the pteroate derivative seemed attractive from a synthetic point of view (fewer synthetic steps), but its tumour uptake is clearly inferior to that of the folate analogues. Significant excretion of our tracer(s) via the hepatobiliary route could hamper their potential for diagnostic application. However, we believe that it is premature to draw final conclusions about the clinical usefulness of $^{99m}\text{Tc}(\text{CO})_3$ -folate tracers in general. Finally, the $^{99m}\text{Tc}(\text{CO})_3$ - γ -folate **4** was successfully assessed in vivo for localisation of FR-positive organs and tissue using one of the first combined small animal SPECT/CT devices installed in Europe. The promising pre-clinical results warrant further investigations in order to assess and improve organometallic ^{99m}Tc folate derivatives for potential use in nuclear medicine.

Acknowledgements. We thank Dr. Ilse Novak-Hofer, Dr. Robert Waibel and Dr. Elisa Garcia-Garayoa for valuable discussions and Alain Blanc, Judith Stahel and Christine De Pasquale for technical assistance. This work was financially supported by Mallinckrodt-Tyco Inc. and Merck Eprova AG.

References

- Miotti S, Canevari S, Menard S, Mezzanzanica D, Porro G, Pupa SM, et al. Characterization of human ovarian carcinoma-associated antigens defined by novel monoclonal antibodies with tumor-restricted specificity. *Int J Cancer* 1987;39:297–303
- Coney LR, Tomassetti A, Carayannopoulos L, Frasca V, Kamen BA, Colnaghi MI, et al. Cloning of a tumor-associated antigen: MOv18 and MOv19 antibodies recognize a folate-binding protein. *Cancer Res* 1991;51:6125–6132
- Weitman SD, Lark RH, Coney LR, Fort DW, Frasca V, Zurawski VR, et al. Distribution of the folate receptor GP38 in normal and malignant cell lines and tissues. *Cancer Res* 1992;52:3396–3401
- Toffoli G, Cernigoi C, Russo A, Gallo A, Bagnoli M, Boiocchi M. Overexpression of folate binding protein in ovarian cancers. *Int J Cancer* 1997;74:193–198
- Parker N, Turk MJ, Westrick E, Lewis JD, Low PS, Leamon CP. Folate receptor expression in carcinomas and normal tissues determined by a quantitative radioligand binding assay. *Anal Biochem* 2005;338:284–293
- Leamon CP, Low PS. Folate-mediated targeting: from diagnostics to drug and gene delivery. *Drug Discov Today* 2001;6:44–51
- Sudimack J, Lee RJ. Targeted drug delivery via the folate receptor. *Adv Drug Deliv Rev* 2000;41:147–162
- Leamon CP, Reddy JA. Folate-targeted chemotherapy. *Adv Drug Deliv Rev* 2004;56:1127–1141
- Li S, Deshmukh HM, Huang L. Folate-mediated targeting of antisense oligodeoxynucleotides to ovarian cancer cells. *Pharm Res* 1998;15:1540–1545
- Leamon CP, Pastan I, Low PS. Cytotoxicity of folate-pseudomonas exotoxin conjugates toward tumor cells—contribution of translocation domain. *J Biol Chem* 1993;268:24847–24854
- Gabizon A, Shmeeda H, Horowitz AT, Zalipsky S. Tumor cell targeting of liposome-entrapped drugs with phospholipid-anchored folic acid-PEG conjugates. *Adv Drug Deliv Rev* 2004;56:1177–1192
- Mathias CJ, Lewis MR, Reichert DE, Laforest R, Sharp TL, Lewis JS, et al. Preparation of ^{66}Ga - and ^{68}Ga -labeled Ga(III)-deferoxamine-folate as potential folate-receptor-targeted PET radiopharmaceuticals. *Nucl Med Biol* 2003;30:725–731
- Mathias CJ, Wang S, Lee RJ, Waters DJ, Low PS, Green MA. Tumor-selective radiopharmaceutical targeting via receptor-mediated endocytosis of gallium-67-deferoxamine-folate. *J Nucl Med* 1996;37:1003–1008
- Mathias CJ, Wang S, Low PS, Waters DJ, Green MA. Receptor-mediated targeting of ^{67}Ga -deferoxamine-folate to folate-receptor-positive human KB tumor xenografts. *Nucl Med Biol* 1999;26:23–25
- Ke CY, Mathias CJ, Green MA. The folate receptor as a molecular target for tumor-selective radionuclide delivery. *Nucl Med Biol* 2003;30:811–817
- Guo WJ, Hinkle GH, Lee RJ. ^{99m}Tc -HYNIC-folate: a novel receptor-based targeted radiopharmaceutical for tumor imaging. *J Nucl Med* 1999;40:1563–1569
- Mathias CJ, Green MA. A kit formulation for preparation of [^{111}In]In-DTPA-folate, a folate-receptor-targeted radiopharmaceutical. *Nucl Med Biol* 1998;25:585–587
- Mathias CJ, Green MA. Alternative kit formulations for compounding of ^{111}In -DTPA-folate (folatescan). *J Nucl Med* 2000;41:1113
- Siegel BA, Dehdashti F, Mutch DG, Podoloff DA, Wendt R, Sutton GP, et al. Evaluation of ^{111}In -DTPA-folate as a receptor-targeted diagnostic agent for ovarian cancer: initial clinical results. *J Nucl Med* 2003;44:700–707
- Leamon CP, Parker MA, Vlahov IR, Xu LC, Reddy JA, Vetzal M, et al. Synthesis and biological evaluation of EC20: a new folate-derived, ^{99m}Tc -based radiopharmaceutical. *Bioconjugate Chem* 2002;13:1200–1210
- Reddy JA, Xu LC, Parker N, Vetzal M, Leamon CP. Preclinical evaluation of ^{99m}Tc -EC20 for imaging folate receptor-positive tumors. *J Nucl Med* 2004;45:857–866
- Alberto R. New organometallic technetium complexes for radiopharmaceutical imaging. In: Krause W, editor. *Contrast agents III: Radiopharmaceuticals—from diagnostics to therapeutics*. Berlin Heidelberg New York: Springer; 2005; p. 1–44
- Boschi A, Duatti A, Uccelli L. Development of technetium-99m and rhenium-188 radiopharmaceuticals containing a terminal metal-nitrido multiple bond for diagnosis and therapy. In: Krause W, editor. *Contrast agents III: Radiopharmaceuticals—from diagnostics to therapeutics*. Berlin Heidelberg New York: Springer; 2005; p. 85–115
- Alberto R, Schibli R, Egli A, Schubiger AP, Abram U, Kaden TA. A novel organometallic aqua complex of technetium for the labeling of biomolecules: synthesis of [$^{99m}\text{Tc}(\text{OH}_2)_3(\text{CO})_3$] $^+$ from [$^{99m}\text{TcO}_4$] $^-$ in aqueous solution and its reaction with a bifunctional ligand. *J Am Chem Soc* 1998;120:7987–7988
- Alberto R, Schibli R, Waibel R, Abram U, Schubiger AP. Basic aqueous chemistry of [$\text{M}(\text{OH}_2)_3(\text{CO})_3$] $^+$ (M=Re, Tc) directed towards radiopharmaceutical application. *Coord Chem Rev* 1999;192:901–919
- Schibli R, La Bella R, Alberto R, Garcia-Garayoa E, Ortner K, Abram U, et al. Influence of the denticity of ligand systems on the in vitro and in vivo behavior of ^{99m}Tc (I)-tricarboxyl complexes: a hint for the future functionalization of biomolecules. *Bioconjugate Chem* 2000;11:345–351

27. Alberto R, Ortner K, Wheatley N, Schibli R, Schubiger AP. Synthesis and properties of boranocarbonate: a convenient in situ CO source for the aqueous preparation of [$^{99m}\text{Tc}(\text{OH}_2)_3(\text{CO})_3$] $^+$. *J Am Chem Soc* 2001;123:3135–3136
28. Schibli R, Schubiger PA. Current use and future potential of organometallic radiopharmaceuticals. *Eur J Nucl Med Mol Imaging* 2002;29:1529–1542
29. Müller C, Dumas C, Hoffmann U, Schubiger PA, Schibli R. Organometallic ^{99m}Tc -technetium(I)- and Re-rhenium(I)-folate derivatives for potential use in nuclear medicine. *J Organomet Chem* 2004;689:4712–4721
30. Antony AC, Kane MA, Portillo RM, Elwood PC, Kolhouse JF. Studies of the role of a particulate folate-binding protein in the uptake of 5-methyltetrahydrofolate by cultured human KB cells. *J Biol Chem* 1985;260:4911–4917
31. Dixon KH, Mulligan T, Chung KN, Elwood PC, Cowan KH. Effects of folate receptor expression following stable transfection into wild type and methotrexate transport-deficient ZR-75-1 human breast cancer cells. *J Biol Chem* 1992;267:24140–24147
32. Ladino CA, Chari RVJ, Bourret LA, Kedersha NL, Goldmacher VS. Folate-maytansinoids: target-selective drugs of low molecular weight. *Int J Cancer* 1997;73:859–864
33. Trump DP, Mathias CJ, Yang ZF, Low PSW, Marmion M, Green MA. Synthesis and evaluation of $^{99m}\text{Tc}(\text{CO})_3$ -DTPA-folate as a folate-receptor-targeted radiopharmaceutical. *Nucl Med Biol* 2002;29:569–573
34. Leamon CP, DePrince RB, Hendren RW. Folate-mediated drug delivery: effect of alternative conjugation chemistry. *J Drug Target* 1999;7:157–169
35. Kamen BA, Wang MT, Streckfuss AJ, Peryea X, Anderson RGW. Delivery of folates to the cytoplasm of MA104 cells is mediated by a surface membrane receptor that recycles. *J Biol Chem* 1988;263:13602–13609
36. Paulos CM, Reddy JA, Leamon CP, Turk MJ, Low PS. Ligand binding and kinetics of folate receptor recycling in vivo: impact on receptor-mediated drug delivery. *Mol Pharmacol* 2004;66:1406–1414
37. Spinella MJ, Brigle KE, Sierra EE, Goldman ID. Distinguishing between folate receptor-a-mediated transport and reduced folate carrier-mediated transport in L1210 leukemia cells. *J Biol Chem* 1995;270:7842–7849
38. Kamen BA, Capdevila A. Receptor-mediated folate accumulation is regulated by the cellular folate content. *Proc Natl Acad Sci U S A* 1986;83:5983–5987
39. Paulos CM, Turk MJ, Breur GJ, Low PS. Folate receptor-mediated targeting of therapeutic and imaging agents to activated macrophages in rheumatoid arthritis. *Adv Drug Deliv Rev* 2004;56:1205–1217
40. Birn H, Spiegelstein O, Christensen EI, Finnell RH. Renal tubular reabsorption of folate mediated by folate binding protein 1. *J Am Soc Nephrol* 2005;16:608–615
41. Morshed KM, Ross DM, McMartin KE. Folate transport proteins mediate the bidirectional transport of 5-methyltetrahydrofolate in cultured human proximal tubule cells. *J Nutr* 1997;127:1137–1147
42. Selhub J, Rosenberg IH. Demonstration of high-affinity folate binding activity associated with brush border membranes of rat kidney. *Proc Natl Acad Sci U S A* 1978;75:3090–3093
43. Goresky CA, Watanabe H, Johns DG. Renal excretion of folic acid. *J Clin Invest* 1963;42:1841
44. Mathias CJ, Wang S, Waters DJ, Turek JJ, Low PS, Green MA. Indium-111-DTPA-folate as a potential folate-receptor-targeted radiopharmaceutical. *J Nucl Med* 1998;39:1579–1585
45. Mathias CJ, Hubers D, Low PS, Green MA. Synthesis of [^{99m}Tc]DTPA-folate and its evaluation as a folate-receptor-targeted radiopharmaceutical. *Bioconjugate Chem* 2000;11:253–257
46. Ke CY, Mathias CJ, Green MA. Targeting the tumor-associated folate receptor with an ^{111}In -DTPA conjugate of pteric acid. *J Am Chem Soc* 2005;127:7421–7426